INITIAL COMMISSIONING OF NDCX-II*

S. Lidia#, D. Arbelaez, W. Greenway, J.-Y. Jung, J. Kwan, T. Lipton, A. Pekedis, P. Roy, P. Seidl, J. Takakuwa, W. Waldron, LBNL, Berkeley, CA 94720, U.S.A
A. Friedman, D. Grote, W. Sharp, LLNL, Livermore, CA, U.S.A.

E. Gilson, PPPL, Princeton, NJ, U.S.A.

Abstract

The Neutralized Drift Compression Experiment-II (NDCX-II) will generate ion beam pulses for studies of Warm Dense Matter and heavy-ion-driven Inertial Fusion Energy. The machine will accelerate 20-50 nC of Li+ to 1.2-3 MeV energy, starting from a 10.9-cm alumino-silicate ion source. At the end of the accelerator the ions are focused to a sub-mm spot size onto a thin foil (planar) target. The pulse duration is compressed from ~500 ns at the source to sub-ns at the target following beam transport in a neutralizing plasma. We first describe the injector, accelerator, transport, final focus and diagnostic facilities. We then report on the results of early commissioning studies that characterize beam quality and beam transport, acceleration waveform shaping and beam current evolution. We present simulation results to benchmark against the experimental measurements.

Figure 1: NDCX-II Facility. The injector is at the far end, with the diagnostic end station at the near end.

NDCX-II BEAMLINE

The NDCX-II facility [1] and beamline is shown in Fig. 1. The machine is composed of a pulsed, electrostatic injector (130kV, ~1µsec FWHM), followed by 27 lattice periods of solenoid (pulsed, 2-3 T) transport, induction cell longitudinal pulse shaping and acceleration, and non-interceptive beam diagnostics. Figure 2 details the position of induction bunching, acceleration, and drift cells, and the final plasma neutralization drift line.

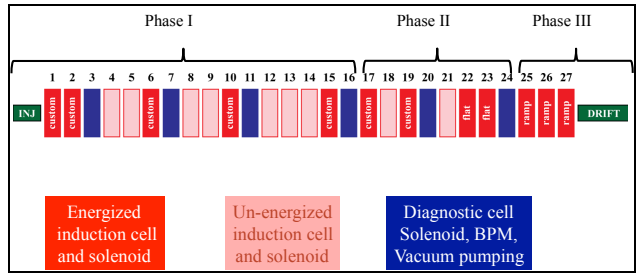

Figure 2: NDCX-II beamline schematic and commissioning phases.

The commissioning phases depicted in Fig. 2 correspond to the relative complexity of the beam dynamics and parameter evolution. This is shown in Fig. 3.

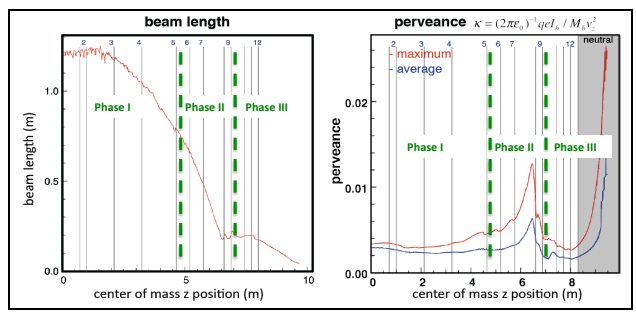

Figure 3: Bunch length and beam intensity (perveance) variation during commissioning phases.

COMMISSIONING STUDIES

We have begun commissioning of the injector and a short (5 cell) beamline to integrate the facility controls, pulsed power, diagnostics, and data acquisition systems. The first series of tests measured the performance and lifetime of the 10.9cm alumino-silicate Li^+ ion source [2,3]. The second series involved demonstration of beam transport and current transmission through 5 cell periods (6 solenoids), including 2 active induction cell gaps, a diagnostic cell, and 2 inactive induction cells.

Source emission

The first source emitter produced over 60 hours of beam at surface temperatures >1250°C. We ultimately measured peak currents of ~60 mA, with ~35nC over ~1µsec [3]. Early performance of the source emitter is

* This work was performed under the auspices of the U.S Department of Energy by LLNL under contract DE AC52 07NA27344, and by LBNL under contract. DE-AC02-05CH11231.
#smlidia@lbl.gov

shown in Fig. 4, which depicts the variation of collected beam charge versus injector extraction voltage and emitter surface brightness temperature.

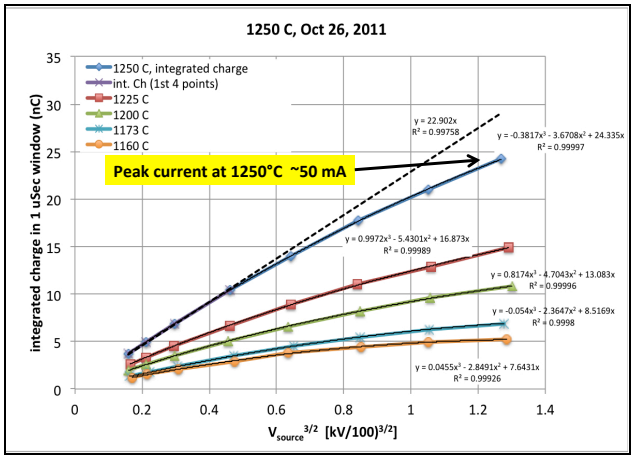

Figure 4: Measured variations in collected beam charge over 1 µsec duration.

Measured current profiles in the diagnostic end station Faraday cup detail the activation of the source emitter over a period of hours. The Li^{+} beam signal is seen to rise as the impurity signal degrades over time. Figure 5 shows a late-time current profile. An ad-hoc Richardson-Dushman thermionic emission model has been used with the WARP simulation code to study multi-species emission and transmission. Time-of-flight measurements indicate K^{+1} as the main impurity component.

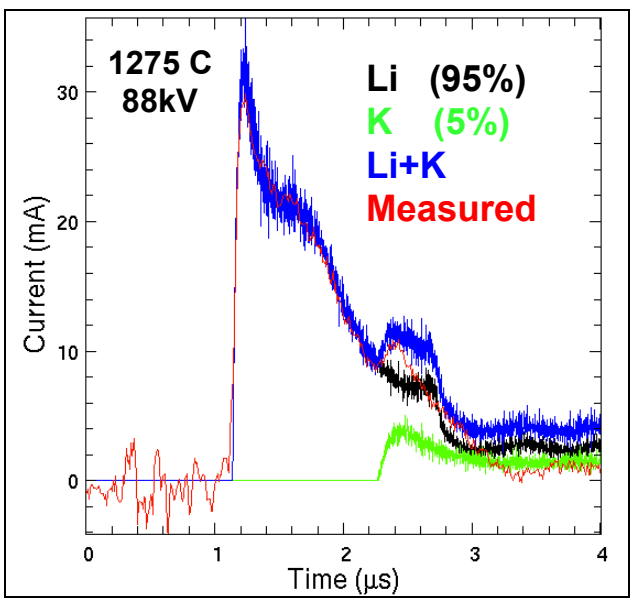

Figure 5: Measured and modeled beam current waveforms at the injector exit.

5-cell test beamline

An initial test beamline has been established for beam transport studies and to begin pulse compression and longitudinal beam manipulation. The 5-cell beamline is shown in Fig. 6. Here, the beam is transported through 5 cell periods (6 solenoids).

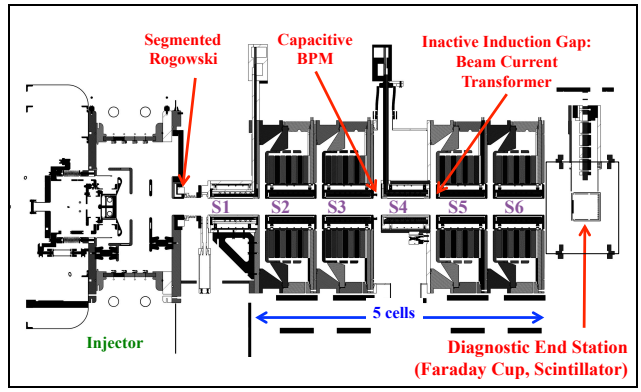

Figure 6: Injector and 5-cell beamline.

Following transport optimization, the beam is accelerated through two active induction cells with tailored waveforms (near S3 and S4 in Fig. 6), and allowed to drift the last 3 periods. The voltage waveforms applied to the beam in the active cells are shown in Fig. 7. The first cell applies an approximately uniform voltage gain, while the second cell applies a time-correlated voltage to begin pulse compression.

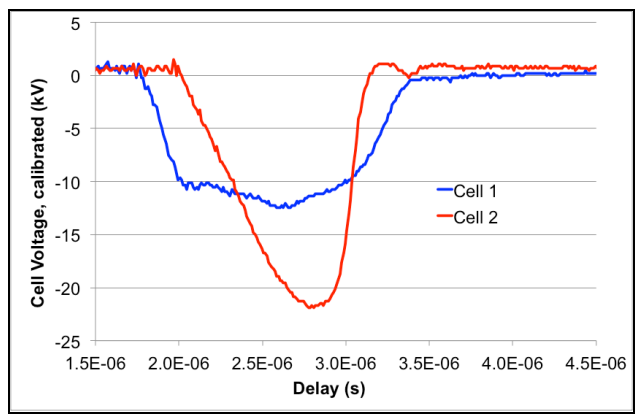

Figure 7: Voltage waveforms of induction cells 1 and 2.

The beam current profiles are measured in the diagnostic end station at the exit of the 5-cell beamline (Fig. 6). We show, in Fig. 8, the results of two sets of measurements. In the first case, the injector extraction voltage was set to 36 kV and extracted a peak current ~15 mA. In the second case, the injector was operated at 112kV with a peak extracted current ~53 mA. The action of the 2 active induction gaps and the following drift line is shown clearly in Fig. 8. The 1-µsec box in Fig. 8 indicates the region of integration for collected charge as well as the gate for optical beam profile measurement.

Beam profile images were acquired with a fast, gated camera and optical scintillator (Al_2O_3). Background-subtracted images are shown in Figure 9 for the 112kV injector voltage case, with and without additional acceleration from the two downstream induction cells.

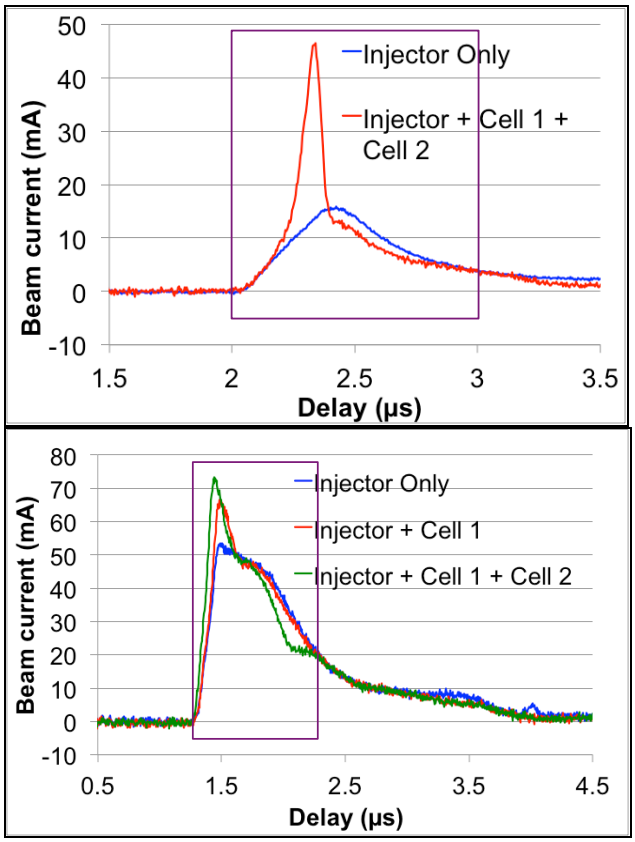

Figure 8: Current waveforms measured at the 5-cell beamline exit. Top: 36 kV injector voltage. Bottom: 112 kV injector voltage.

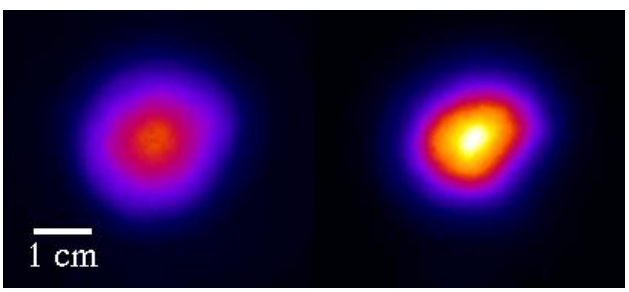

Figure 9: Beam image at injector voltage 112kV. Left: after 5-cell transport only. Right: after 5-cell transport and acceleration by 2 induction cells.

The beam pulse energy, peak fluence, and beam spot size have been measured and inferred from the Faraday cup and beam profile images, for both the 36kV and 112kV injector voltage cases. The values are listed in Table 1.

This work was supported by the Director, Office of Science, Office of Fusion Energy Sciences, of the U.S. Department of Energy under Contract No. DE-AC02-05CH11231.

Present Status and Future Work

Currently, the machine is being readied for Phase-Ia of the commissioning series. This will involve an 11-cell beamline with 4 active induction cells for pulse compression and shaping.

New diagnostics have been fabricated and installed in the diagnostic end station. The present beam diagnostic suite now includes a deep (10 cm) Faraday cup, optical scintillator, plus two sets of movable slit and slit-Faraday cup paddles for time-resolved phase space density measurements. Crossed slit measurements are also possible, to complete the measurements necessary for complete beam matrix determination, but may suffer from unacceptable electronic noise level.

Upcoming work will concentrate on improving source performance to achieve space charge limited flow at the highest injector extraction potentials, reducing the growth of corkscrew modes in beam transport, and tuning the induction cell waveforms for optimum longitudinal pulse compression.

Table 1: Beam parameters at diagnostic end station.

$V_{injector}$ (kV)	36	112
Beam Pulse Energy (mJ)		
Injector only	0.5	4.4
Injector + 2-cells	0.6	4.7
Peak beam fluence (mJ/cm^2)		
Injector only	0.11	1.2
Injector + 2-cells	0.14	2.3
Beam diameter, FWHM (mm)		
Injector only	16	18
Injector + 2-cells	13	13

REFERENCES

[1] J.W. Kwan, et al., “NDCX-II, an Induction Linac for HEDP and IFE Research”, GSI HEDP Annual Report as 2010 HIF Symp. Proc.
[2] P.A. Seidl, et al., "Development and testing of a lithium ion source and injector", Phys. Rev. ST Accel. Beams 15, 040101 (2012).
[3] P.K. Roy, et al., these proceedings.

DISCLAIMER

This document was prepared as an account of work sponsored by the United States Government. While this document is believed to contain correct information, neither the United States Government nor any agency thereof, nor the Regents of the University of California, nor any of their employees, makes any warranty, express or implied, or assumes any legal responsibility for the accuracy, completeness, or usefulness of any information, apparatus, product, or process disclosed, or represents that its use would not infringe privately owned rights. Reference herein to any specific commercial product, process, or service by its trade name, trademark, manufacturer, or otherwise, does not necessarily constitute or imply its endorsement, recommendation, or favoring by the United States Government or any agency thereof, or the Regents of the University of California. The views and opinions of authors expressed herein do not necessarily state or reflect those of the United States Government or any agency thereof or the Regents of the University of California.